Structural Analysis of Historical Constructions – Jerzy Jasieńko (ed)
© 2012 DWE, Wrocław, Poland, ISSN 0860-2395, ISBN 978-83-7125-216-7

ASSESSMENT OF THE CAPACITY OF MONDIM DA BEIRA BRIDGE USING TWO DISTINCT MESH GENERATIONS

Morais M.J.C.[1], *Rouxinol G.A.F.*[2], *Pimenta P.J.R.*[3]

ABSTRACT

The aim of this paper is to present a numerical analysis concerning a roman masonry arch bridge named Mondim da Beira. The bridge is located in Portugal, Tarouca – Mondim da Beira and the analysis is performed using a Discrete Element Method (DEM) with plane rigid elements developed by the second author. The main objective is to compare the estimation value of the load capacity of the roman bridge through two distinct mesh generations. One is obtained automatically reading the span and the rise of the arch, whereas the other approach reads each stone of the arch through a topographical survey. For this two mesh generations concerning two 2D models were considered. The first one is constituted by the isolated arch with vertical actions simulating the fill. The second one considers the arch with a spandrel wall. The estimation of the 3D value of the load capacity results from the combination of both solutions. The material properties adopted in the analysis are those found in the specialized Study Case bibliography. Finally, the advantages of using each mesh generation are presented.

Keywords: *Discrete element method, Bridge, Mesh generation, Collapse masonry, Arch*

1. INTRODUCTION

The numerical analysis presented in this paper is part of a work developed in the Master of Science Course of Construction and Rehabilitation Engineering at the School of Management and Technology of Viseu (ESTGV), Portugal, entitled "Masonry arch bridge – Study Case". The masonry arch bridge in analysis concerns the roman bridge of Mondim da Beira at Tarouca, Portugal, with two well distinct spans. To this work, the adopted computational program consists in the use of two-dimensional mixed discrete element program LFE-MEDM [1]. The computer program includes two kinds of elements: polygonal and circular. Nonetheless, only polygonal elements are considered here.

The main goal of the analysis is to compare the estimation value of the load capacity of the bridge (particularly for the largest arc), using two distinct meshes of polygonal discrete elements. One mesh was derived from topographical surveys, referred to as Case I, and another mesh was obtained by means of an automatic generation, referred to as Case II. To each of those cases two models of the load structure are studied: (a) Model 1 – isolated arch plus vertical dead loads applied in the extrados of the arch, simulating the material filling the arch; and (b) Model 2 – arch plus spandrel walls of the arch. In both models, explicitly or implicitly, the dead load was considered and a incrementally load of knife kind located at one fourth of the arch span was applied. This concentrated load was gradually incremented until the collapse of the structure was reached. The analysis was performed per meter width of the bridge and the estimation of the 3D value of the load capacity results from the combination of both models. The material properties adopted in the analysis are those considered in the specialized bibliography. Finally, the advantages of using each mesh case of polygonal discrete elements are presented.

[1] Master Student, Polytechnic Institute of Viseu, mariajcmorais@gmail.com
[2] Assistant Professor, INESC Coimbra & Polytechnic Institute of Viseu, rouxinol@estv.ipv.pt
[3] Civil Engineer, Câmara Municipal de Tarouca, paulocmtarouca@hotmail.com

2. DESCRIPTION OF THE BRIDGE

The bridge is a medieval bridge of Romanesque architecture, whose construction was held, probably, between the thirteenth and fourteenth centuries [2]. The bridge has a regular typology with granite block stones with unfilled joints. It has its foundation in a rocky outcrop of granite, which is partially hidden by works that intend to recreate a river beach and occupies the margins where the arch bridge is constructed. The bridge consists of two arches that are unequal in size and in typology (Fig. 1). Above there is a roadway with safety guards made with stones. The largest arch has a shape that resembles a perfectly round, whereas the smallest arch has a shape similar to a pointed arch. In the visual inspection carried, the main structural damage observed was a considerable deformation of the largest arch.

The bridge has a length of about 56.5 m, a height of approximately 11.9 m (vertical dimension in the coating zone of the largest arch) and a width of 4.8 m. The largest arch has a span of 15.7 m, the rise of the midspan is of 7.2 m and the average thickness of the sandstone voussoir possesses 1.0 m. The distance from the keystone extrados of the largest arch to the roadway is inexistent. On Fig. 1, the downstream elevation survey and the cutting coating section of the largest arch are shown.

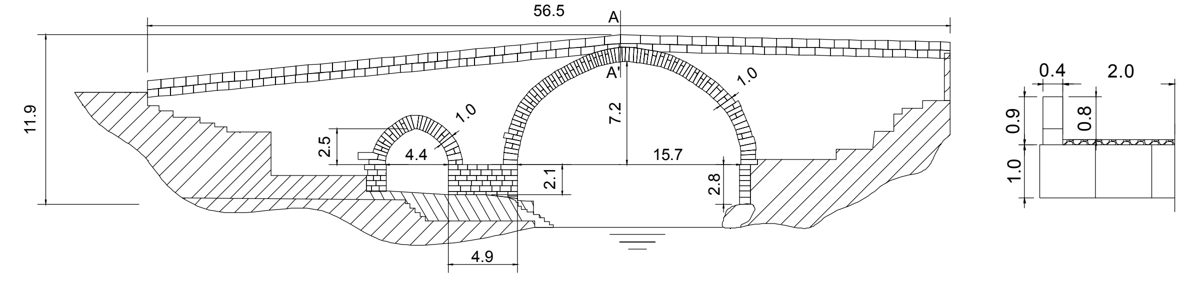

Fig. 1 Romanic bridge of Mondim da Beira: (a) downstream elevation; (b) section AA' (drawings are not to scale)

3. GENERAL CONSIDERATIONS

3.1. Mechanical characteristic of materials

It is noted that since there are not tests performed to the materials constituting the bridge, one adopted the mechanical characteristics of such materials proposed in the specialized literature. Therefore, the values of the maximum compressive stress of the masonry units, f_b, the Poisson's ratio, ν_b, and the modulus of elasticity, E_b, report the values adopted by Costa [3]. For the density of the masonry units, ρ_b, and the maximum tensile stress of the masonry units, f_{bt}, one considered the value used by Rouxinol [1]. Table 1 lists the mechanical material properties of the bridge. For the value of the shear modulus of the masonry units, the well-known relationship $G_b = 0.5E_b/(1+\nu_b)$ was used.

Table 1 Mechanical properties of the masonry units

f_b (MPa)	f_{bt} (MPa)	E_b (GPa)	ν_b	G_b (GPa)	ρ_b (kg/m^3)
43.80	5.00	15.00	0.20	6.25	2100.00

As the composition of the filling of the bridge is not known, it was adopted a mixture of gravel, sand and clay with a density ρ_f = 1890 kg/m^3 and a deformability modulus E_f = 40.0 MPa, according to Rouxinol [1]. The joints were assumed to follow a linear elastic "perfectly plastic" constitutive model governed by the Coulomb slip criterion, neglecting cohesion. For the friction angle, one adopted 36 degrees, following Vieira [4], and, for the contact tangential stiffness, a value equal to 0.4 of the contact normal stiffness value was considered.

For the maximum tensile stress of the joint, it was assumed a value equal to zero. For the maximum compressive stress of the joint, it was considered the value equal to the maximum tensile stress of the masonry units, f_b. For the normal contact stiffness, kn, a range of values equal to 1, 10 and 100 GPa/m were adopted.

3.2. Consideration about the DEM solution

For this analysis, the following considerations about the solution of the discrete element method were taken: the formulation of the discrete element method is made in terms of forces, i.e., the influence length of the punctual contact is fixed; the damping for the solution method concerns a local damping equal to 0.8; the rounding distance of the discrete element corners is fixed at 1.0 cm. The influence length of the point contact is equal to half of the average thickness of the voussoirs minus the rounding distance. Other numerical parameters of the DEM, like the coefficient for the time step and coefficients that measure / activate the routine of the detection contact and update of the contact, are considered by default. For more details about the DEM solution see [5].

3.3. Dead load and incremental live load

The DEM itself accounts the self-weight of the masonry units and, therefore, it is not necessary to input its value. However, the self-weight of the material filling of the arch is not accounted and must be inserted by applying a dead load in the extrados vertex of the masonry units of the arch. For this purpose and as the DEM only allows automatic dead load data for horizontal roadway, the dead load was calculated through the combination of a Excel sheet with AutoCad drawings (see Fig. 2). Thus, the self-weight of the slice above the extrados masonry units of the arch and below the roadway was evaluated and spread to their vertexes. Fig. 2 also shows the dead load applied vertex numeration and Fig. 3 shows their arrows.

As stated previously, the incremental live load was applied to one fourth span of the arch with an increment of 10 kN until the collapse is reached. The section at one fourth span is one of the most unfavorable locations of the load application. In the cases I and II the live load was applied in two extrados vertexes of the discrete element 31 and 44, respectively. The non-symmetric black line relative to the vertical line that cross the center of the semi-circular arch is due to the non-horizontal roadway: the roadways in the left and in the right possess different slopes.

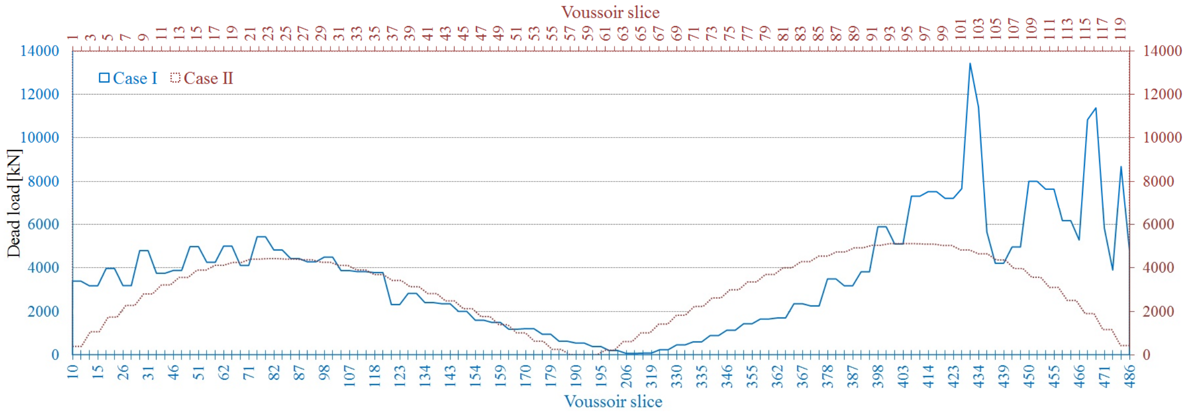

Fig. 2 Dead loads of the model 1: blue line for case I and broken red line for case II

3.4. Generation mesh

The characterization of the geometry of the bridge was obtained through a topographical survey performed by a designer and a survey technician of the City Hall of Tarouca. The final drawing of the bridge was recorded in a digital AutoCad dxf file. To reproduce the mesh of discrete elements for case I, it was necessary to draw over each masonry unit of the dxf file, respecting a determined sequence. After this procedure, the new dxf file is read by the LFE-MEDM program (see Fig. 3). For case II, the LFE-MEDM program has some routines that allow the automatic generation of several standard structural elements such as the semi-circular arches and spandrel walls with some adaptation, making the compatibility between the discrete elements of extrados arch and the discrete elements of the spandrel walls (Fig. 3). The difference of the elevation between each generation is about 0.62 m (see Fig. 4).

4. NUMERICAL ANALYSIS

The purpose of this section is to report the four analyses carried, namely, for cases I and II with each one of them using models 1 and 2, assessing the bearing capacity load of the bridge. As stated above, it was considered for each model a range of three different values for the contact stiffness of the point contact, kn (1, 10 and 100 GPa/m). The displacement read / measured is the displacement of the mass center of the discrete element that supports the incremental load. When it is mentioned the "ultimate load" it means that it is still supported by the structures, i.e., the collapse load is represented by this load plus an incremental load.

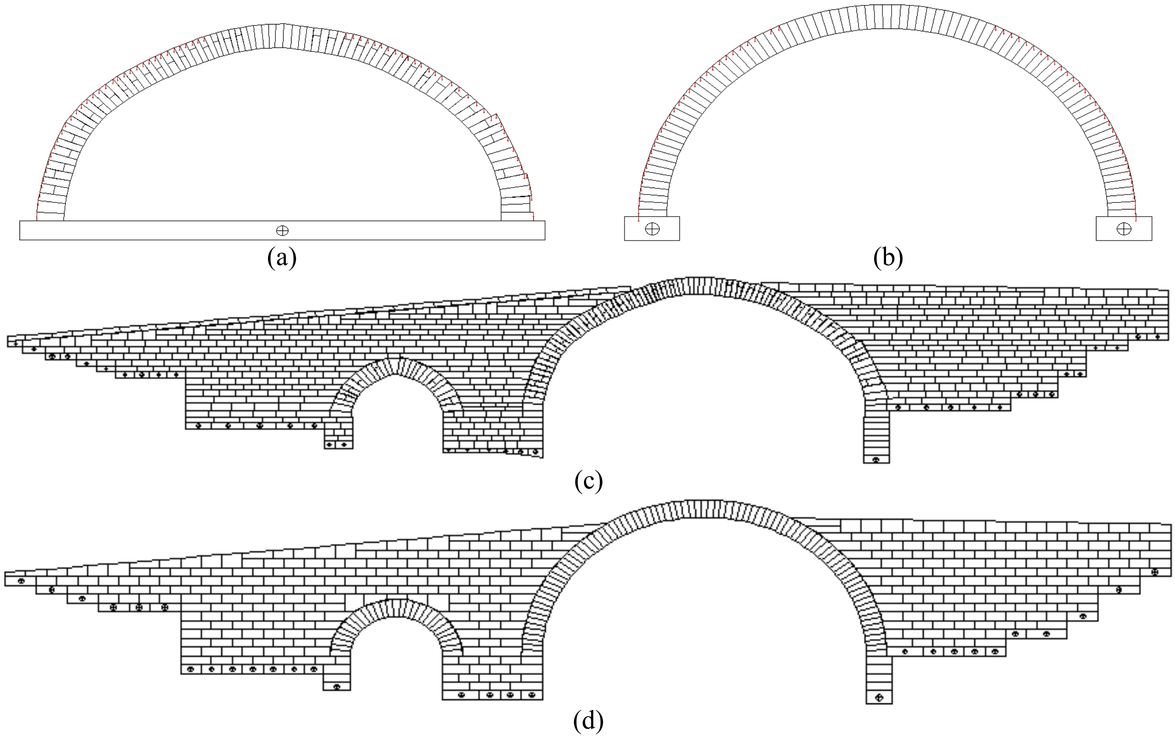

Fig. 3 Generation mesh and arrow dead loads: (a) and (c) case I; (b) and (d) case II

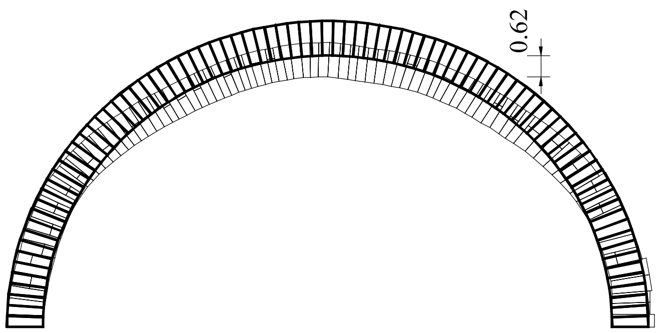

Fig. 4 Elevation difference between each generation: case I and II (in meters)

4.1. Analysis of the Case I – Topographical Survey

4.1.1. Model 1 – Isolated Arch

Once the analysis of the case I through the model 1 was performed, it was concluded that for the first and third stiffness ranges the model is more ductile and rigid, respectively (as can be seen in Fig. 8). The initial displacements due to the dead load only for the three ranges of the stiffness contact are 17.90, 1.85 and 0.20 mm. The ultimate loads for the three ranges of the stiffness contact are 132, 162 and 162 kN and the displacements are 87.01, 10.28 and 1.02 mm, accordingly. There is an increased load of about 22.7% between the first and the other two ranges of the stiffness contact and a decreased displacement of about 89.9% between the 2nd and 3rd ranges of the stiffness contact. Concerning the stress values, for the 1st and 2nd ranges of the stiffness contact, the maximum value is lower than 1.5 MPa at the contact point 2 until the 8th increment load and is lower than 1.6 MPa at the contact point 301 for the remaining increment. For the 3rd range of the stiffness contact, similar stresses are perceived; nevertheless, the maximum stress at the last increment load is 1.7 MPa. The contact point 2 is located between the fixed and the first left discrete element of the arch (extrados side), and the contact point 301 is located between the fixed and the last right discrete element of the arch (extrados side), see (Fig. 5).

4.1.2. *Model 2 – Full Arch*

Once the analysis of the case I through the model 2 was performed, it was concluded that for the first and second stiffness ranges the model is more ductile and rigid, respectively (as can be seen in Fig. 8). The initial displacements due to the dead load only for the three ranges of stiffness contact, are 11.64, 1.27 and 0.15 mm. Due to the high rigidity of this structure, the analysis crashed for the model with the 3rd range of the stiffness contact (kn = 100 GPa/m) at about one half of the LFE-MEDM run.

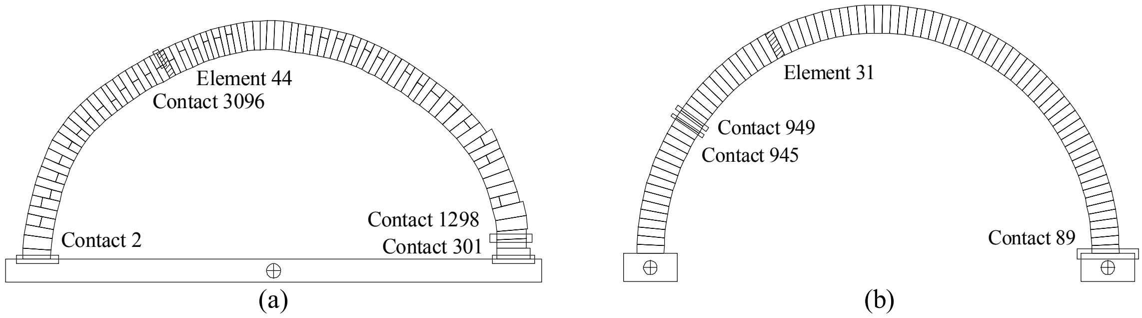

Fig. 5 Localization of some local contact points: (a) case I; and (b) case II

The large overlap at some local specific points might be the source of the crash. Consequently, this model is outcast. The ultimate loads for the two ranges of the stiffness contact are 535 and 684 kN, and their displacements are 95.31 and 16.04 mm, accordingly. There is an increased load of about 27.8% between the first and the second range of the stiffness contact and a decreased displacement of about 83.2% between the 2nd and 3rd ranges of the stiffness contact. Concerning the stress values, for the 1st and 2nd ranges of the stiffness contact, the maximum value is lower than 0.8 MPa at the contact point 1298 until the 13th and 14th increment load, respectively, and is lower than 2.5 and 2.7 MPa, respectively, at the contact point 3096 for the remaining increment. The contact point 1298 is located between two right discrete elements of the arch next to the support (extrados side), and the contact point 3096 is located between two discrete elements of the arch where one of them supports the load (extrados side), see Fig. 5.

4.2. Analysis of the Case II – Automatic Generation

4.2.1. *Model 1 – Isolated Arch*

In the same way to the case I model 1, the analysis of the case II through model 1 lead us to conclude for the first and third stiffness ranges that the model is more ductile and rigid, respectively (as can be seen in Fig. 8). The initial displacements only due to the dead load for the three ranges of the stiffness contact are 15.23, 1.50 and 0.15 mm. The ultimate loads for the three ranges of the stiffness contact are 127, 143 and 144 kN, and their displacements are 59.82, 6.40 and 0.64 mm, accordingly. There is an increased load of about 12.6% between the first and the two other ranges of the stiffness contact and a decreased displacement of about 90.0% between the 2nd and 3rd ranges of the stiffness contact. Relatively to the stress values, for all the ranges of the stiffness contact, the maximum value is always lower than 1.5 MPa at the contact point 89, from the first to the last incremental load. The contact point 89 is located between the fixed and the last right discrete element of the arch (extrados side), see Fig. 5.

4.2.2. *Model 2 – Full Arch*

Once the analysis of the case II through the model 2 was performed, it was concluded for the first and third stiffness ranges that the model is more ductile and rigid, respectively (as can be seen in Fig. 8). The initial displacements due to the dead load only, for the three ranges of the stiffness contact, are 10.90, 1.08 and 0.11 mm. The ultimate loads for the three ranges of the stiffness contact are 601, 715 and 760 kN, and their displacements are 86.39, 13.43 and 2.53 mm, accordingly. There is an increased load about 26.5% between the 1st and 3rd ranges of the stiffness contact and a decreased displacement of about 81.2% between the 2nd and 3rd ranges of the stiffness contact. Relatively to the stress values, for the 1st range of the stiffness contact, the maximum value is always lower than 1.7 MPa at the contact point 949, from the first to the last increment load. For the 2nd and 3rd ranges of the stiffness contact, the maximum value is lower than 2.0 MPa at the contact point 949 until the 71st and 73rd incremental load, respectively, and it is lower than 2.5 MPa at the contact point 945 for the remaining increment. The contact points 945 and 949 are located between two discrete elements at the middle left height of the rise of the arch (intrados side), see Fig. 5.

5. ANALYSIS OF THE RESULT

The (Fig. 8) shows the load-displacement relations for all models of cases I and II. Given Table 1, the maximum compressive stress values obtained in all models are lower than the maximum compressive stress. The configuration of the incipient effective collapse obtained for models 1 and 2, in all ranges of the stiffness contact, is the expected mechanism of collapse of this type of structures at 4 hinges located alternatively between the intrados and the extrados (see Fig. 6 and Fig. 7). The capacity load of the 3D bridge can be approximated, for cases I and II (Load I and Load II), considering the collaboration of models 1 and 2, by combining the corresponding results. This combination can be made taking into account their relative stiffness or, for simplicity, taking the proportion of their relative widths (fill 4.0 m and spandrel wall 0.8 m), see Table 2.

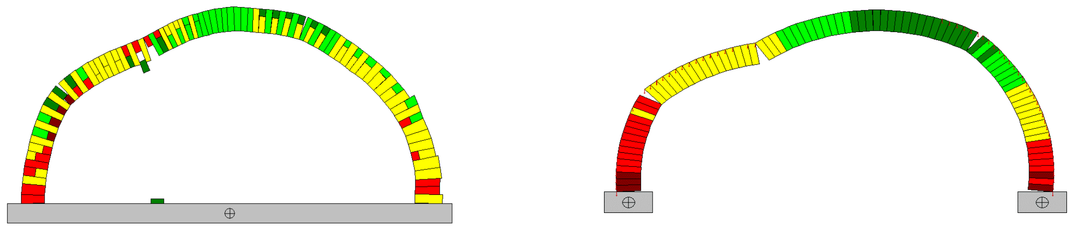

(a) (b)

Fig. 6 Collapse mechanism (kn = 1 GPa/m): (a) Case I; (b) Case II

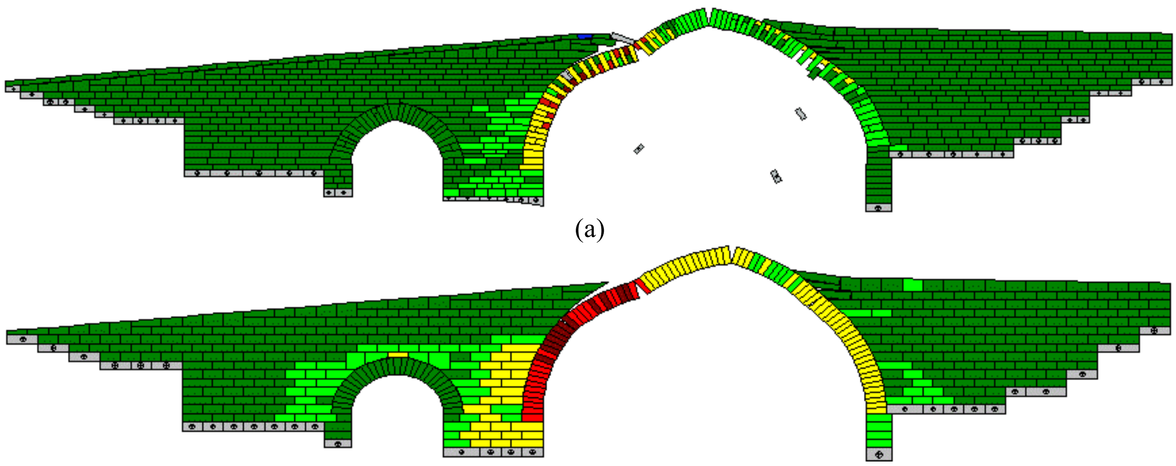

(a)

(b)

Fig. 7 Collapse mechanism (kn = 10 GPa/m): (a) Case I; (b) Case II

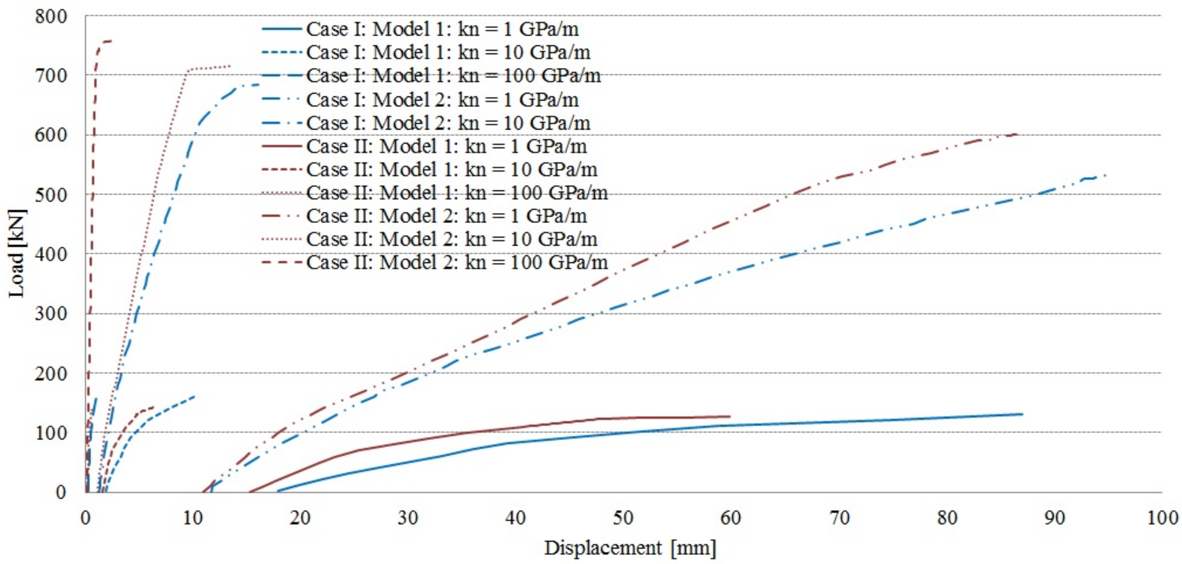

Fig. 8 Load-displacement relations for all cases and models

Table 2 Capacity load of the 3D bridge

kn (GPa/m)	Load I (kN)	Load II (kN)
1	199.2	206.0
10	249.0	238.3
100	---	246.7

6. CONCLUSIONS

This communication compares the estimation of the load capacity value of the roman bridge Mondim da Beira through two distinct mesh generations. The discrete element method was used for the numerical computation. Since the mechanical characteristics of the materials are not known, some values obtained in the specialized literature were considered. Other values were taken by adopting a certain range of values for the rigidity stiffness of the local punctual contact.

It is shown that the two meshes significantly lead to the same values of the capacity load (Table 2). It is not visible a good standard split-up between both approaches. Therefore, adopting a combination coefficient, γ_Q , of 1.5 and adopting the minimum value of the capacity load obtained, the capacity load provides a load of 132.8 kN (= 199.2/1.5).

ACKNOWLEDGEMENTS

The authors thank the President Mario Caetano Ferreira of City Hall of Tarouca for the celebration of the Protocol, the designer Paulo Trindade and the survey technician Carlos Barros, both of City Hall of Tarouca, for the drawing of the bridge and to Tiago Abreu, professor at ESTGV, for the relevant suggestions and support.

REFERENCES

[1] Rouxinol, G. (2007) Modelação e Avaliação Estrutural de Pontes em Arco de Alvenaria. Coimbra: Faculdade de Ciências e Tecnologia da Universidade de Coimbra. PhD Thesis.

[2] Instituto de Gestão do Património Arquitectónico e Arqueológico, www.igespar.pt. [Online] [Citation: 9 August 2011].

[3] Costa, C. (2002) Análise do Comportamento da Ponte da Lagoncinha sob a Acção do Tráfego Rodoviário. Porto: Faculdade de Engenharia da Universidade do Porto. Master' Thesis.

[4] Vieira, M. (1997) Um Modelo de Elementos Discretos para o Estudo de Estruturas de Alvenaria. Lisboa: Instituto Superior Técnico da Universidade Técnica de Lisboa. Master' Thesis.

[5] Rouxinol, G., Providência, P., Lemos, J., (2006) The discrete elemento method with 2D rigid polygonal and circular elements. In P.B. Lourenço, P. Roca, C. Modena, S. Agrawal (Eds.) *Structural Analysis of Historical Constructions*, New Delhi.